Landslides (2014) 11:513–525
DOI 10.1007/s10346-013-0453-x
Received: 14 January 2013
Accepted: 27 November 2013
Published online: 21 December 2013

Bolin Huang · Yueping Yin · Shichang Wang · Xiaoting Chen · Guanglin Liu · Zhibing Jiang · Junzhe Liu

A physical similarity model of an impulsive wave generated by Gongjiafang landslide in Three Gorges Reservoir, China

Abstract Landslide-related impulse waves are catastrophic but accidental, so limited data on field measurements are available; scaled physical experiment is therefore a functional method to simulate and analyze this phenomenon. A large-scale physical Froude-similar model to produce impulse waves was constructed based on the Chinese Gongjiafang landslide, which occurred on the main stream of Three Gorges after the impounding in the reservoir in China. With a scale of 1:200, the model had the dimensions of 24, 8, and 1.3m. Four water levels, 145, 156, 172.8, and 175m, were modeled for the experiments, and marble coarse sands were used to imitate the actual cataclastic rock mass. Wave height gauges, high-speed cameras, and run-up measuring instruments were used to monitor wave fluctuations in the model. Among the experiments, the ones modeled using a water level of 172.8m best confirmed the actual conditions in the Gongjiafang landslide, representing a good validation of the experiments. This study obtained, for the first time, specific data on the reproduced impulse waves' convergence and superposition during propagation, and of the energy change between impulse waves and reflected waves. The test data describe a rapid decaying and gradual decaying rule for the wave heights and run-ups. The Froude-similar experiments presented in this article help us to understand the whole procedure of impulsive wave generated by cataclastic rock mass failure, and the results acquired contribute to studies of impulse waves caused by similar bank destabilizations worldwide.

Keywords Froude-similar experiment · Three Gorges Reservoir of China · The Gongjiafang landslide · Cataclastic rock mass · Impulse wave

Introduction

Historically, catastrophic impulse waves on rivers, lakes, and reservoirs caused by collapsing, landslides, debris flows, lava flows, and volcanic ash flows have been recorded around the world (Alvarez-Cedrón et al. 2009; Silvia et al. 2011; Yang 1987; Huang et al. 2012; Wang et al. 1986; Yin et al. 2008; Fritz 2002). Impulse waves, as a nonlinear and highly complicated phenomenon, require interdisciplinary study using geological engineering, geological disaster kinematics, hydraulics, fluid dynamics, etc. Nevertheless, as geological hazards, impulse wave are extremely rare, and the effects of the water on the surrounding banks disappear after the waves occur. Instant measurements of impulse waves in the field are thus limited, and the study of impulse waves, as a result, is challenging. Considering the complication of limited data on impulse waves, physically similar experiments can be a functional solution (Heller et al. 2009).

Previously, scientists around the world have carried out physical modeling of impulse waves using generalized models such as block model (Kamphuis et al. 1970; Ataie-Ashtiani et al. 2008), granular slide models (Wieland et al. 1999; Ursell et al. 1960; Fritz et al. 2001), and piston models (Hughes 1993; Synolakis 1991; Sander 1990). By combining various slopes and types of impulse waves, the researchers also studied the run-ups of the waves (Fritz et al. 2001; Hall et al. 1953; Gedik et al. 2005). However, those generalized models were simplified models (Marcello et al. 2009), so some complex but crucial factors were omitted, and the connections between all of the parts of the impulse wave process were ignored, so the conclusions were relatively less persuasive. Compared to the above models, a scaled model offers more detailed observations and accurate data on the formation, propagation, and run up of impulse waves while taking the main factors of the real conditions into consideration. Moreover, those data are connected and better for systematic analysis. A prototype scaled experiment is an outstanding method to rebuild, and even pre-visualize, the entire processes of the impulse waves intuitively and to collect abundant precise data (Heller et al. 2009).

Because of the huge expense, large area occupied, time required, and massive data associated with a physical model, it is not a widely applied method. At the Western Canada Hydraulic Laboratories, using a scale of 1:300, Ball (1970) simulated impulse waves related to a potential landslide into Columbia Mica Reservoir in the UK, using a gravel bag model. In 1974, using iron cases as the slide mass, Davidson and Whalin (1974) created a physical model of impulse waves on Montana Koocanusa Lake at a scale of 1:120 and predicted landslides in multiple locations around the lake. Later, Huber and Hager (1997) reanalyzed the data from the previous two experiments and deduced a formula for calculating impulsive wave propagation. Muller and Schurter (1993) duplicated the planar clastic grain flows and its impulse waves on the Urnersee River. To meet the design requirements of Three Gorges Dam, in early 1984, the Chinese Yangtze Valley Planning Office of Water Conservancy and Electric Power Ministry performed some physical similarity experiments and analysis of several typical landslides along the river upstream of the dam. One example is the Xintan landslide; many statistics on run-up were gained when postulating two distinctive collapsed slide masses, 5 and 16 million cubic meters (Liu 1987). Another example is the 1:150-scale model of impulse waves from the Lianziya dangerous rock mass of China (Wang et al. 1994). In the experiments, more than 80 potential conditions were tested using various slide masses, and mixed sliding rates, and three flow rates for the river. Using dimensionless analysis, formulae for calculating maximum wave height and for impulse wave

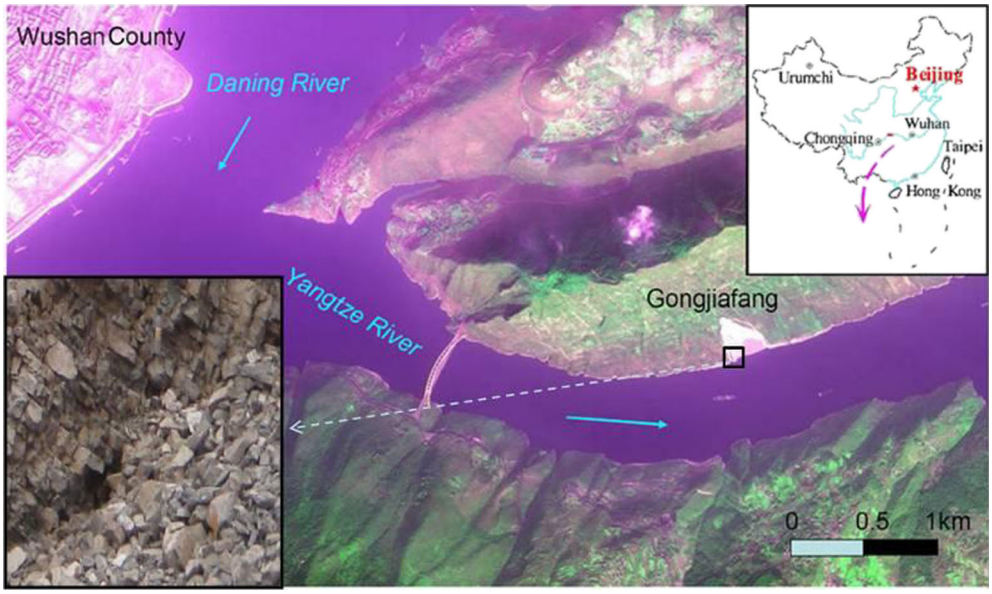

Fig. 1 A remote sensing image of the landslide area from INKOS data gathered in March 2009. A map (*upper right*) shows the location of Gongjiafang, and the *lower left photo* shows its rock mass structure

propagation were deduced from the statistics obtained from the experiments.

Although the above studies and research have generally demonstrated the wave height regularity of impulse waves resulting from the destabilization of rock and soil masses, detailed processes were not shown effectively. There has been almost no previous research on scaled physical experiments of impulse waves associated with destabilization of cataclastic rock masses in China. There is thus little information on the construction of cataclastic rock mass prototypes, their validity, and rules. In this article, prototype scale experiments of cataclastic rock mass destabilization were carried out based on the Gongjiafang landslide (November 23, 2008). Four various water levels, 145, 156, 172.8, and 175 m, were selected to use in the experiments. In addition, the formation, propagation, and run-ups of the following impulse waves in varied conditions were analyzed. Statistics and methods in this article contribute to the understanding of impulse waves caused by the collapse of disaggregated rock masses in gorges.

An overview of the Gongjiafang landslide

Located within the Three Gorges Reservoir of China, the Gongjiafang slope along the Changjiang River is 4.5 km downstream from Wushan County, Chongqing City and is at the entrance of Wu Gorge (Fig. 1). The bedrock of the slope is chiefly early Triassic, mainly group 3 (T_1d^3) and group 4 (T_1d^4) of the Daye Formation plus group 1 (T_1j^1) of the Jialingjiang Formation (Fig. 2). Most of the bedrock is thin sheets of marlstone, limestone, and dolomitic limestone mixed with shale, with a strike of 350–353° and a dip of 44–47° (Fig. 2). There are two major structural planes developed in the rock mass with attitudes of 130–170°∠40–60° and 210–240°∠70–85° that crosscut the layers, making the rock mass blocky (Fig. 1).

The Gongjiafang slope as a whole dips to the southeast with an original slope angle of 54°. The landslide mass on the ridge was bounded by two nearby gullies; altitudes of the landslide toe and head scarp are 100 and 380 m, respectively. After the collapse, the fresh surface had a shape of an isosceles trapezoid, with a height of 293 m, widths of 45 m on the top, and 194 m at the foot. The vertical height of the landslide mass was 210 m (Fig. 2). By comparing the landscapes before and after failure, it is calculated that the sliding direction was 160° and the sliding area was 25,178 m^2, with an average thickness of 15 m and a total volume of 380,000 m^3. The sizes of collapsed blocks were measured over a

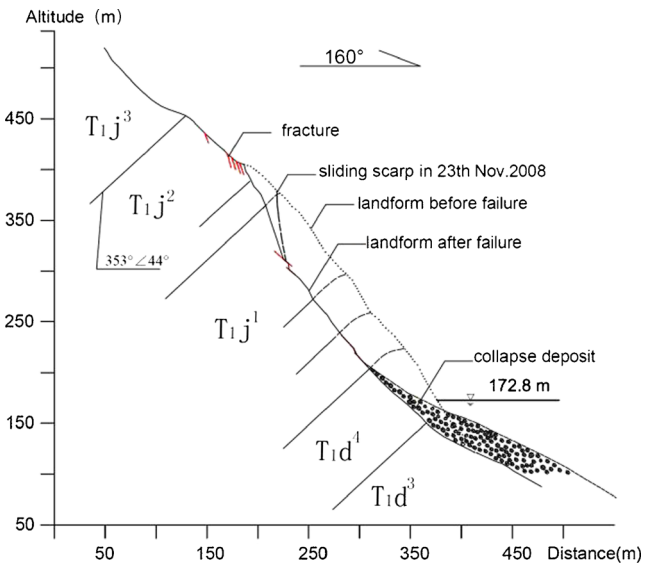

Fig. 2 Geo-engineering section of Gongjiafang slope

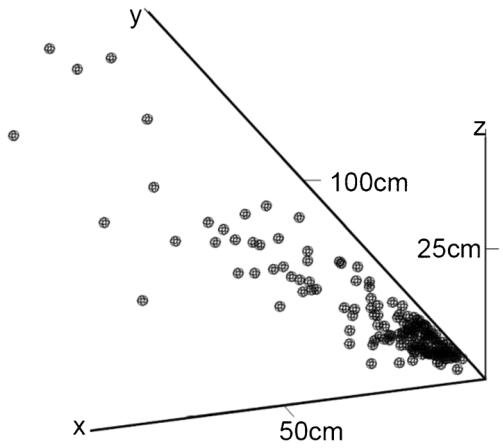

Fig. 3 Map of distribution of 176 blocks' sizes

2 m×2-m area for statistical analysis. One hundred seventy-six blocks were measured, and 80 % of them fall into ranges of 20±5 cm length, 8±4 cm width, and 3±2 cm thickness (Fig. 3). The block area measured was a representative area, where blocks were neither too big nor too small. Based on the measured values and field conditions, the authors believe that a mean particle diameter of about 25 cm is reasonable.

The original altitude of the water level in Wu Gorge was about 90 m, and the riverbed had a minimum elevation of approximately 30 m. However, on November 23, 2008, the water level in Wu Gorge was measured to be 172.8 m after impounding, and the breadth of the Changjiang River at Gongjiafang became 480 m. According to surveys conducted by the authors and their collaborators on November 24, 2008, the run-up of the impulse waves on the opposite bank of the landslide reached 12 m and decreased to 1.1 m at Yushan Dock of Wushan County, 4.5 km upstream of the landslide (Fig. 4) (Huang et al. 2012).

For more detailed information about Gongjiafang landslide and the resulting impulsive wave, refer to Huang et al. (2012).

Methods used in the physical experiments

Production of the model

With a scale of 1:200, the physical model of the Gongjiafang landslide mass and impulse waves was produced based on the Froude criterion of gravitational similarity. According to the Froude gravitational similarity law, when the geometric scale is 1:200, the time scale is $1:\sqrt{200}$, the velocity scale is $1:\sqrt{200}$, the density scale is 1, and other physical quantities can be analogous.

The scaled model had a length of 24 m and resembled a 4,800-m stretch of the river from 4,000 m upstream to 800 m downstream of the landslide location. The actual altitudes of the landscape ranged from 30 to 220 m, while in the model, the total height was 1.3 m, with a 0.2-m layer of sands preset at the base and an extra 0.1 m for security reasons on top. The breadth of the model was 8 m (Fig. 5). The model gorge landscape was surfaced with cement mortar and was produced based on contour lines with intervals of 10 m. At the collapse location, the slope of the landscape beneath water level was set to be 54°, which is the average of the Gongjiafang slope underwater.

Using the same scale, an isosceles trapezoid-shaped model of the destabilized landslide mass was made with a higher base of 0.225 m, a lower base of 0.97 m, a vertical height of 1.47 m, and a thickness of 0.075 m. Because of the cataclastic structure of the

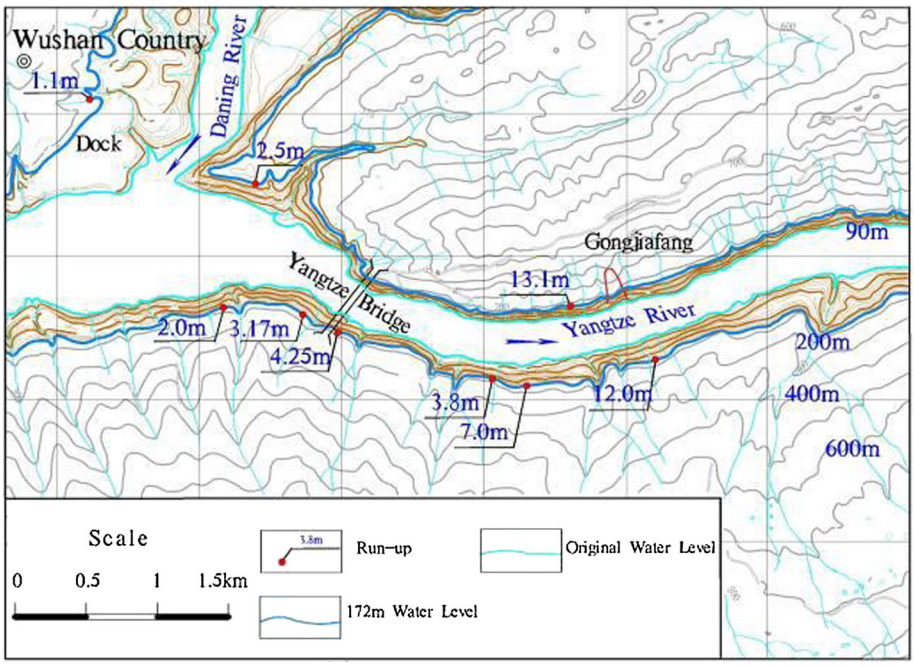

Fig. 4 Run-up conditions of the Gongjiafang impulse wave on November 23, 2008

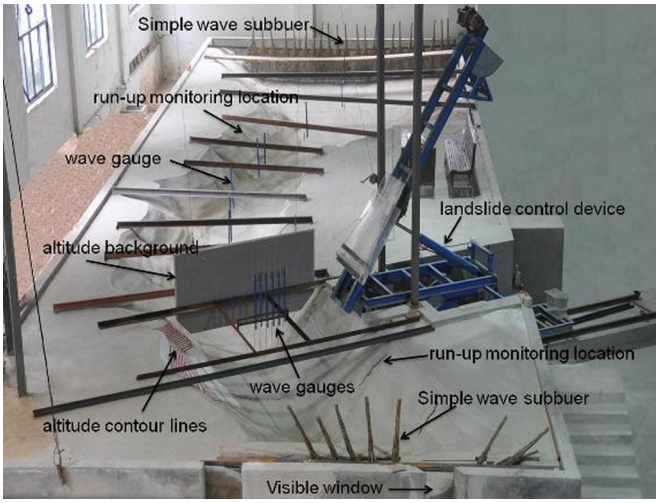

Fig. 5 Valley model and test equipment photo

Gongjiafang slope, when it failed, the landslide mass reached the water as a rocky debris flow. In the experiments, granular rock particles were used to simulate the cataclastic rock mass on the slope. According to Froude law, when the rock block D50 size in the field is 25 cm, the simulation material D50 size is 1.25 mm. A variety of different kinds of materials and particles were compared before marble coarse sand was selected for the experiments. Its density similarity is very good; the density of marble is 2,600 kg/m^3, while limestone and dolomite density is 2,500–2,700 kg/m^3. Sieve analyses showed that the marble particles had a D50 of 1.47 mm, composed of 99.1 % coarse sands (0.5–2 mm) and 0.9 % fine sands (<0.5 mm), fitting the basic principles of similarity generally (Fig. 6).

Testing system of the experiments

In the scaled model, the collapse-simulating device was designed to control the motion of the slide mass so that the precise location

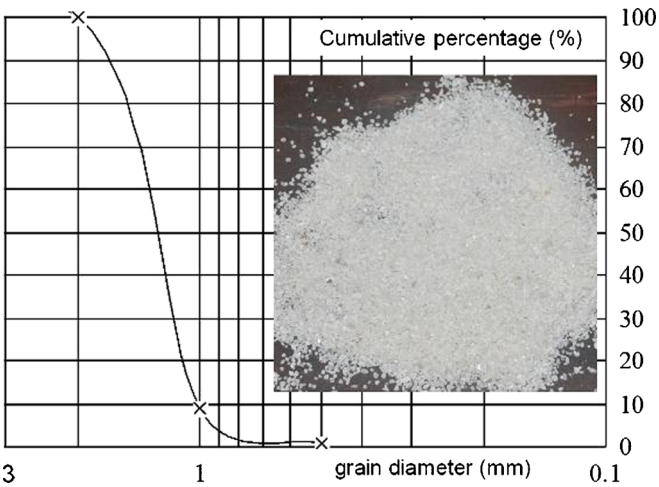

Fig. 6 Similar material and its grain composition curve

Fig. 7 Photo of the collapse stimulating device

of the collapse and the angle of the slope could be adjusted effectively (Figs. 5 and 7). In the device, the slide mass was towed by a motor, the still water level was measured by a water-level point gauge, and the slide slot with a maximum load capacity of 300 kg was connected to a hydraulic system which could rotate the slot and move it horizontally and vertically.

In addition, with an error of ±0.2 mm (model value), six wave height gauges marked 1#–6# were spaced every 12 cm (model value) along the slide route in the river to sharply capture the height of the wave. The background to the model was textured with 5 mm×5 mm squares placed 1 m (model value) above the water upstream of the collapse (Fig. 5) and a 500-fps camera installed at a window in the downstream boundary wall to record the formation of the impulse waves.

At the location opposite the collapse, contour lines with intervals of 0.01 m (model value) were printed on the bank within an area of 2 m (model value) in width and 0.7–1 m (model value) in elevation range. Also, a camera was installed 1 m (model value) downstream to record the run up of the waves on that bank.

To record the effects of the variation of the channel geometry on the propagation of the impulse waves, 9 wave height gauges numbered 7#–15# were positioned upstream along the river's

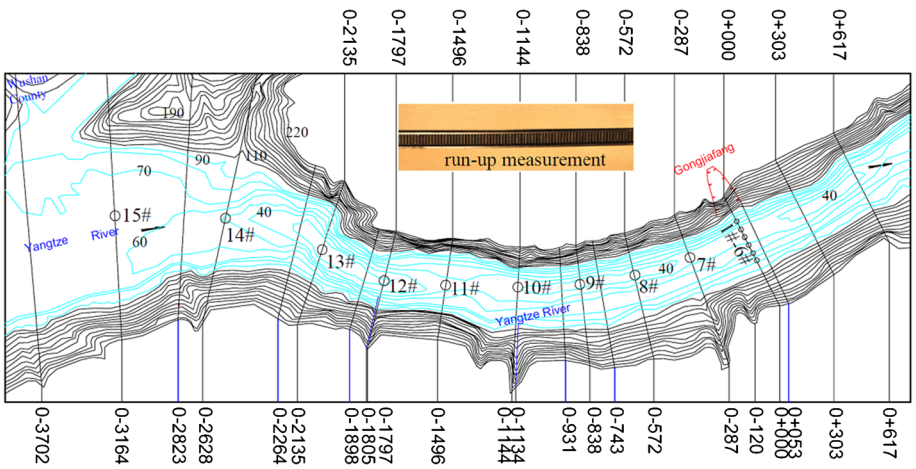

Fig. 8 Locations of wave height gauges and photo of run-up measuring instruments

thalweg to monitor the entire propagation of the impulse waves. The gauge at the collapse location was assigned a station ID 0+000 m, and the station IDs of the other gauges were respectively 0–287 m, 0–572 m, 0–838 m, 0–1,144 m, 0–1,496 m, 0–1,797 m, 0–2,135 m, 0–2,628 m, and 0–3,164 m (see Fig. 8 for detailed locations).

In addition, 15 run-up monitoring locations, including both ridges and gullies, were selected on each bank of the river, with station IDs of 0+617 m, 0+303 m, 0−120 m, 0−287 m, 0−572 m, 0−838 m, 0−1,134 m, 0−1,144 m, 0−1,496 m, 0−1,797 m, 0−1,805 m, 0−2,135 m, 0−2,628 m, 0−3,164 m, and 0−3,702 m. Also, 0.5 mm banding run-up measuring instruments placed on banks (Fig. 8) and leveling instruments were available to measure the run-ups of the impulse waves along the river.

Purpose and plans of the experiments

The primary purposes of the experiments were to

(1) Revisualize the entire formation of the impulse waves generated by the Gongjiafang landslide and verify the validity of the scaled model.
(2) Get more information on the effects of the riverway's landscapes and water level on impulse wave formation, propagation, and run-ups.
(3) Provide basic statistics and technical support for analyzing the damage to banks by impulse waves within 3,000 m of the Gongjiafang landslide.

Based on the goals of the experiments, four groups of experiments were proposed, using different water levels. The levels were 172.8 m to reproduce the level at the time of the Gongjiafang landslide, and 145 m, 156 m, and 175 m for the minimum, normal, and maximum water level of Three Gorges Reservoir. Two repeated experiments were designed for each group of experiments, and the averages of the two sets of data confirming each other were regarded as the result of the experiment.

Estimating the impact velocity of the granular centroid

When a granular mass is sliding into water, the centroid velocity of the moving mass is hard to obtain. The difficulty lies on confirming the location in space of the centroid in the movement and measuring its movement in the air and underwater. Progress in this field is still relatively slow. Fritz (2002) and Heller (2007) studied impulsive waves generated by granular masses with the help of LDS (laser distance sensors), PIV (particle image velocimetry), CWG (capacitance wave gauges), and high-speed cameras. To analyze the impact velocity of the landslide, they used a calculation formula of Körner (1976) (Eq. 1).

$$V_s = \sqrt{2g\Delta z_{sc}(1-\tan\delta\cot\alpha)} \tag{1}$$

where, V_s is centroid impact velocity (meters per second), g is acceleration of gravity (meters per square second), Δz_{sc} is the height between original centroid and still water level (meter), δ is dynamic friction angle, α is slip plane angle. Here, in this experiment, δ is 45°, α is 54°.

Equation 1 ignores the resistance of water and air, resulting in a value for the centroid velocity that is inevitably bigger and thus can be used only for reference. When the water level was 172.8 m, the granular mass centroid height (Δz_{sc}) was 83.2 m. Correspondingly, the Δz_{sc} were 81, 100, and 111 m, respectively, when the water level was 175, 156, and 145 m. Through the formula in Eq. 1, the impact velocity of the granular mass centroid diving into water can be evaluated. The impacting velocities were 20.8, 21.1, 23.2, and 24.4 m/s, respectively, when the water levels are 175, 172.8, 156, and 145 m.

In 2012, using data from a field video, Huang (2012) calculated that the impact velocity of the sliding mass was 12 m/s. So the impact velocity in the 172.8 m water level test should be close to the prototype.

Experiment analyses

The 172.8-m water-level experiment results and validity check

In order to understand the experiment result better, the result data below were converted from model values according to Froude

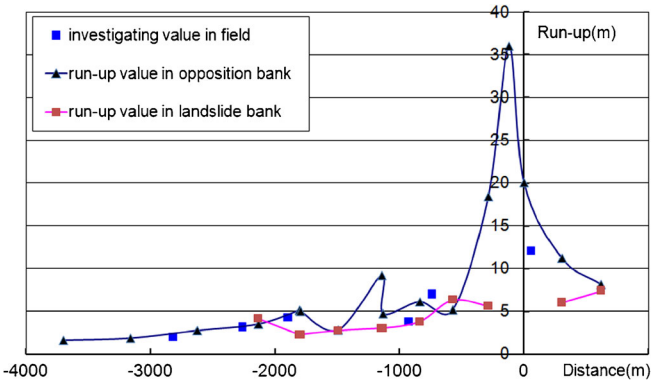

Fig. 9 Contrast of experiment results and survey statistics

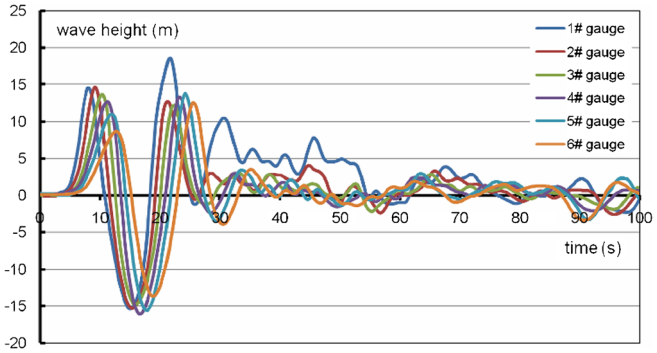

Fig. 10 Wave height process lines of 1#~6# wave gauges in failure direction in a 172.8-m test

gravitational similarity law. From the experiments, at a water level of 172.8 m, impulse waves caused by granular particles had a maximum height of 17.4 m. At the location opposite the collapse, the maximum run-up was 20 m on the ridge and 36 m in the gully.

Because few measurements were made when the landslide occurred on November 23, 2008, the data used to validate the experiments were from post-event surveys. Figure 9 compares the experimental results at a water level of 172.8 m with the survey data. Except for the run-up value of 12 m opposite the collapse, the other survey statistics generally agree with the experiment results, with a correlation coefficient of 0.949 between the two sets of data, with an error less than 10 %.

With the help of a field video, Huang (2012) concluded that the maximum wave height in the riverway may have been 31.8 m. This is the same magnitude to that indicated in the experiment, although there is a 14.4-m difference in height between the two. There may be two main reasons: (1) scale effects in the physical test may cause the maximum wave height to be on the low side and (2) the actual maximum wave goes by a flash, and at that time the ratio of wave height and wave width is very large; it thus may be too difficult to discern with cameras and gauges, resulting in false impressions that the wave is spindrift. This may make the maximum wave height low too. Huang (2012) carried out a numerical simulation on impulsive waves; this paper mainly describes and analyzes physical experimental data, and there is no scale comparsion analysis between the physical experiment data and the numerical simulation data.

In general, the physical experimental data is validated by the high correlation coefficient and small error difference value.

Processes of the impulse waves generated by a granular mass

Although the heights of impulse waves varied for different water levels, the mechanisms of the formation, propagation, and running up of impulse waves are uniform, and some conclusions could be made from the scaled experiments. The gauges data obtained from tests in the water levels of 175, 156, and 145 m can be seen in Appendix Figs. 14, 15, and 16.

(1) Propagation of impulse waves in the direction of rock mass sliding

It was shown for all four water-level groups that two major wave crests for the impulse waves resulted from the collapse of the cataclastic rock mass (Fig. 10). Through analysis of camera images, it was found that the first wave crest was generated before the slide mass entirely entered the water, while the second wave crest was produced after that and sometimes even after the majority of the rock mass had stopped. After the two wave crests were fully created, the impulse waves were still propagating chiefly in the sliding direction of the slide mass. Correspondingly, the wave height gauges numbered 1#–6# set in the sliding direction were designed to monitor the wave heights of these impulse waves.

One example is the impulse waves recorded by the 1#–6# wave height gauges at the water level of 172.8 m (Fig. 10). After the two major wave crests, the impulse waves largely decayed, and the waveforms became more complicated. The more complicated waveform after about 30 s results from constructive and destructive interference of the two original waves and their reflected waves. Due to the limited width of the river in the sliding direction and the long wavelength of the impulse waves, after two wave crests were produced (usually around 20 s), the front of the waves had already reached the opposite bank and triggered reflected waves. At the time of 40 s, the wave forms overlap, although the wave has not yet reached to other areas of the river course (except in the impact area). Thus, at the location where the impulse waves were initiated, the reflected waves also appeared earliest, making the overlapping conditions and waveforms most complex. Meanwhile, the amplitude of the waves was significantly reduced because of superposition in the various wave directions, resulting in the most rapid decay in this area.

(2) Propagation of impulse waves along the river

The propagations and interactions of the impulse waves are shown by the wave height gauges along the thalweg

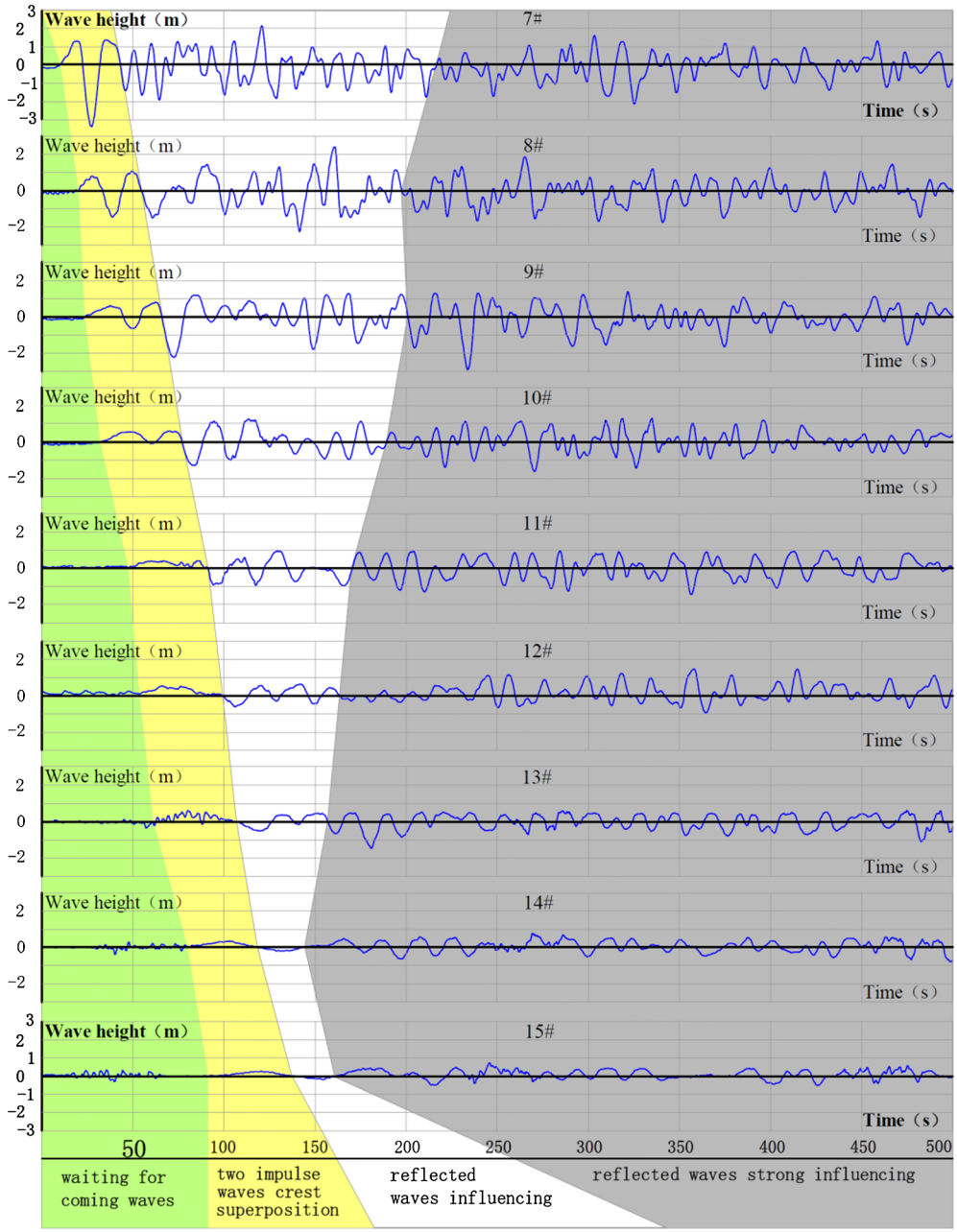

Fig. 11 Wave height process lines of 7#~15#wave gauges in test for a 172.8-m water level

marked 7#–15#. Because of the conformity within the experimental results from the four groups, analysis can be based on solely the experiments for the water level of 172.8 m (Fig. 11).

Figure 11 uses four color areas that represent four stages in the surge process; the stages change slowly. The green region represents the peaceful periods of the river before the waves arrive, and the yellow region is for the propagation and superposition of the first two wave crests with the increase of distance along the river. The two impulse wave crests were propagating and decaying upstream separately until they reached near the #12 wave height gauge (0–1,797 m) and combined into one wave. The combined wave later continued propagating and decaying in the upstream direction.

Reflected waves occurred when the impulse waves reached the banks and later joined the propagation of the original waves. The white region in Fig. 11 displays the circumstances when the reflected waves started to join the propagation. At this time, the energy of impulse waves was greater than that of the reflected waves, and the waveforms were therefore mostly shapes of wave groups. While the amplitudes and general shapes of the wave groups were similar to those of

the original waves, the period of the envelopes was larger. Even though the original impulse waves were affected by reflected waves, they still dominated.

The gray region in Fig. 11 illustrates the heights and shapes of waves formed by the superposition of impulse waves and reflected waves with fairly equal energy. After propagating and decaying for some time, the original waves with greatly reduced energy could no longer form wave groups with reflected waves. The waves tend to have unstable periods, with overall higher frequencies, decreased amplitudes, and more complex and irregular waveforms. In this period of time, the reflected waves had considerable influences on the impulse waves and gradually began to predominate.

In the record from each wave height gauge, it is found that the initial two impulse waves are simple, with a great amplitude and long period (over 30 s). Gradually, the two waves seem to overlap, and small sways are visible in the big wave shape. When the two major waves are superposed on each other, the waveform tends to be complicated, while the amplitude tends to be relatively stable. After a further overlapping of the ring waves, the waveform becomes tangled and even broken; the amplitude is unstable, and the frequency had obviously increased. The wave height gauges perfectly recorded not only the chasing and overlapping of the waves but also the energy change and interaction of the impulse waves and reflected waves.

The chasing of the first two wave crests could be explained by the difference in wave celerity. The celerities could be calculated using the movement of the wave crests from pictures taken by the high-speed cameras. Respectively, the celerities of the first and the second impulse waves were 40–60 and 20–25 m/s in a region near the collapse (0+000 to 0−287 m), 29–35 and 21–30 m/s in a region far from the collapse (0–287 to 0–1,496 m), and 24–40 m/s further away from the collapse (0–1,496 to 0–3,164 m). It was noticeable that along the riverway, the celerity of the first impulse wave was decreasing while that of the second wave was increasing. The two waves therefore overlaped around the location 0–1,797 m.

The impulse wave decay rate can be defined as the ratio of the percentage decay of the wave amplitudes and the propagation distance. Based on the data, the decay of the impulse waves was rapid in the collapse area and slowed with distance away from the collapse. In detail, the impulse wave decay rates for the first two waves were 47.6–56.1 and 26.1–45.4‰ near the collapse (0+000 to 0−287 m) and 0.6–1.2 and 0.5–1.2‰ far from the collapse (0–287 to 0–1,496 m). While further away from the collapse (0–1,496 to 0–3,164 m), the decay rate of the overlap wave was 0.1–0.5‰. With a river width of around 500 m, the region near the collapse was an area of rapid decay, where the decrease of wave height is 5 m over a distance of 100 m. With the increasing distance, the decrease of wave height became 0.1 m over a distance of 100 and 0.05 m in a region at a further distance, called the gradual decaying area (Wang et al. 2003; 2004; Huang et al. 2012).

(3) Run-ups of the impulse waves

As shown in Figs. 12 and 13, with increasing distance from the disturbance area, the maximum run-ups of the impulse waves were generally decreasing. However, the decrease was not a steady decline because the maximum run-up at a location was determined by not only the maximum wave height and the propagation direction of the impulse waves but also by the microrelief of the landscape in the shallow water nearby. Hence, the distance of propagation can only partially influence the run-ups along the river. It was also obvious that the maximum run-ups always occurred in the gully opposite the collapse. Run-ups in concave landscapes like gullies were generally higher than those on nearby convex landscapes like ridges. One explanation is that after an impulse wave entered a concave landscape and was trapped, the transmission of energy was constrained horizontally and thus turned to potential energy vertically.

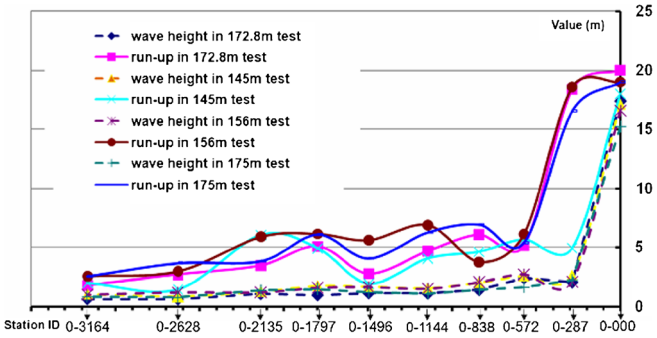

Fig. 12 Variation of wave heights and run-ups in four water-level groups

In addition, it was observed that the wave heights at the thalweg locations were lower than contemporary run-ups on the banks (Fig. 12). The theory for run-ups in concave landscapes applies to this phenomenon as well. Locations along the thalweg were the deepest places in the river. When the impulse waves were propagating from these locations toward the banks, the deepness of the water decreased, and the horizontal transmission of energy was limited by the underwater landscape, so the excess energy was transmitted vertically, resulting in the differences between run-ups and wave heights.

On the basis of the graph in Fig. 12, it can be predicted that the analysis of rapidly decaying and gradual decaying

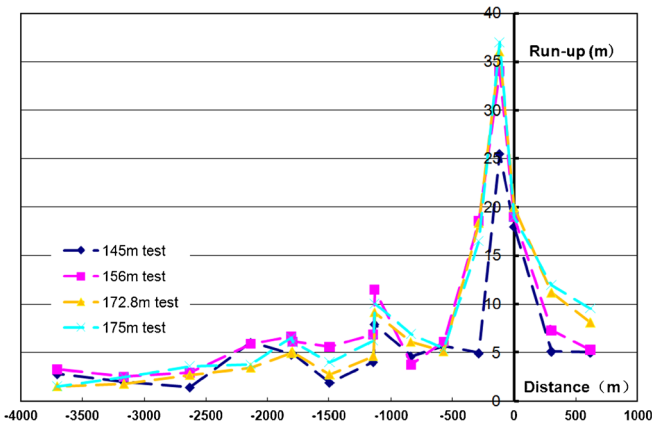

Fig. 13 Run-ups at different water levels

Table 1 List of impulse wave heights in different water levels

Water level (m)	The first wave crest		The second wave crest		Max. run-up value in 0+000 station (m)	Max. run-up value in riverway (m)
	Height (m)	Decay ratio (‰)*	Height (m)	Decay ratio (‰)*		
145	17.10	50.4	9.60	26.1	18.0	25
156	16.59	50.5	12.83	39.1	19.0	34
172.8	17.40	56.1	14.40	45.4	20.0	36
175	15.20	47.6	12.00	36.0	19.0	37

*Decay ratio measured the decay from 0 to 287 m

waves was also compatible with the run-ups of the impulse waves because of the decay with distance (Wang et al. 2008; Dai et al. 2008). Nevertheless, unlike the propagation of the waves, the run-up was sensitive to the microrelief, especially in concave landscapes like gullies. Associated with the change of landscape, the decay of run-ups did not follow a simple decay schedule and so was not easy to qualify.

Variation in impulse wave height with different water levels

The first and second wave crest heights of impulse waves for different water levels are presented in Table 1. With the still water depth and impact velocity changing, the heights of impulse waves changes. The results are not strictly consistent with previous knowledge (Ataie-Ashtiani and Nik-Khah 2008), which was that with the rise in the water level, the wave crest height decreases. There may be two main reasons: the landslide mass dynamic control and the wave height obtained are the two major technical difficulties in the experiments. Although repeated tests were used to improve the precision of the data, it was impossible to avoid test error. When the water level rose from 145 to 175 m, the fluctuation of the heights of impulse waves was within 2.2 m, about 14.5 %.

When examining the run-ups at the location opposite the collapse (station ID 0+000 m), a slight increase was found with the rise of water level. Moreover, the maximum run-ups usually occurred in a gully (station ID 0–120 m) on the opposite side of the collapse, and this run-up increased with the water level. Specifically, when the water level rose 30 m, run-up at the gully location with station ID 0+000 m grew 5.56 %, and the maxima run-up in the river grew about 48 %. With the 30 m water-level rise, the average change was about 4.49 % on the other bank of the riverway except the gullies (Fig. 13).

Conclusions and suggestions

Using the Froude criterion of gravitational similarity, a large physically similar scale model of impulse waves in a reservoir associated with destabilization of a cataclastic rock mass was constructed based on the Chinese Gongjiafang landslide in Three Gorges Reservoir, using coarse marble sand (D50= 1.47 mm), to imitate the slide mass. Four water levels, 145, 156, 172.8, and 175 m, were selected for the experiments. In the experiments, equipment that included high-speed cameras, wave height gauges, and run-up measuring instruments were used to monitor the waves.

In the revisualizing experiments of the Gongjiafang landslide with a water level of 172.8 m, the maximum wave height of the impulse waves was 17.4 m in the riverway; the maximum run-up was 20 m on the ridge opposite the collapse, and 36 m in the nearby gully. With a correlation coefficient of 0.949 and a deviation less than 10 %, the results agreed with field-survey statistics. The experiments with a 172.8-m water level closely represented the actual reservoir conditions at the time of the Gongjiafang landslide.

Wave height gauges were able to record the entire process of impulse wave propagation in the riverway and the energy changes of the impulse and reflected waves. They recorded that after the two biggest impulse wave crests were produced in the collapse, they started to propagate and the distance between them decreased, so that they later combined and finally were superimposed with their reflected waves. The experimental data detailed the characteristics of impulse wave propagation and decay rates. With the increase of distance from the source, rapid decaying and gradual decaying areas were shown to exist for wave heights and run-ups of the impulse waves. With the water level rose, the wave height and run-up had difference in changing rate.

These physical experiments on impulse waves enabled detailed and accurate visualization of the formation of the impulse waves caused by the slide mass in the gorge river landscape, and provide useful reference and technical support for research on impulse waves that might result from rapid failure of other unstable slopes around Gongjiafang and elsewhere.

Acknowledgments

This work was funded by the China Geological Survey (project ID: 1212011014027) and National Natural Science Foundation of China (project ID: 41372321). We would like to express our gratitude to our friends: Prof. Guangze Peng and Prof. Fei Ma from Chongqing Three Gorges Reservoir Geological Hazards Prevention and Control Office for supplying us with necessary data. We also want to thank Prof. Jibing Han from Yangtze River Scientific Research Institute for giving us helpful suggestions. Finally, we appreciate some anonymous reviewers and Dr. Mauri McSaveney; they gave good suggestions on the manuscript.

Appendix

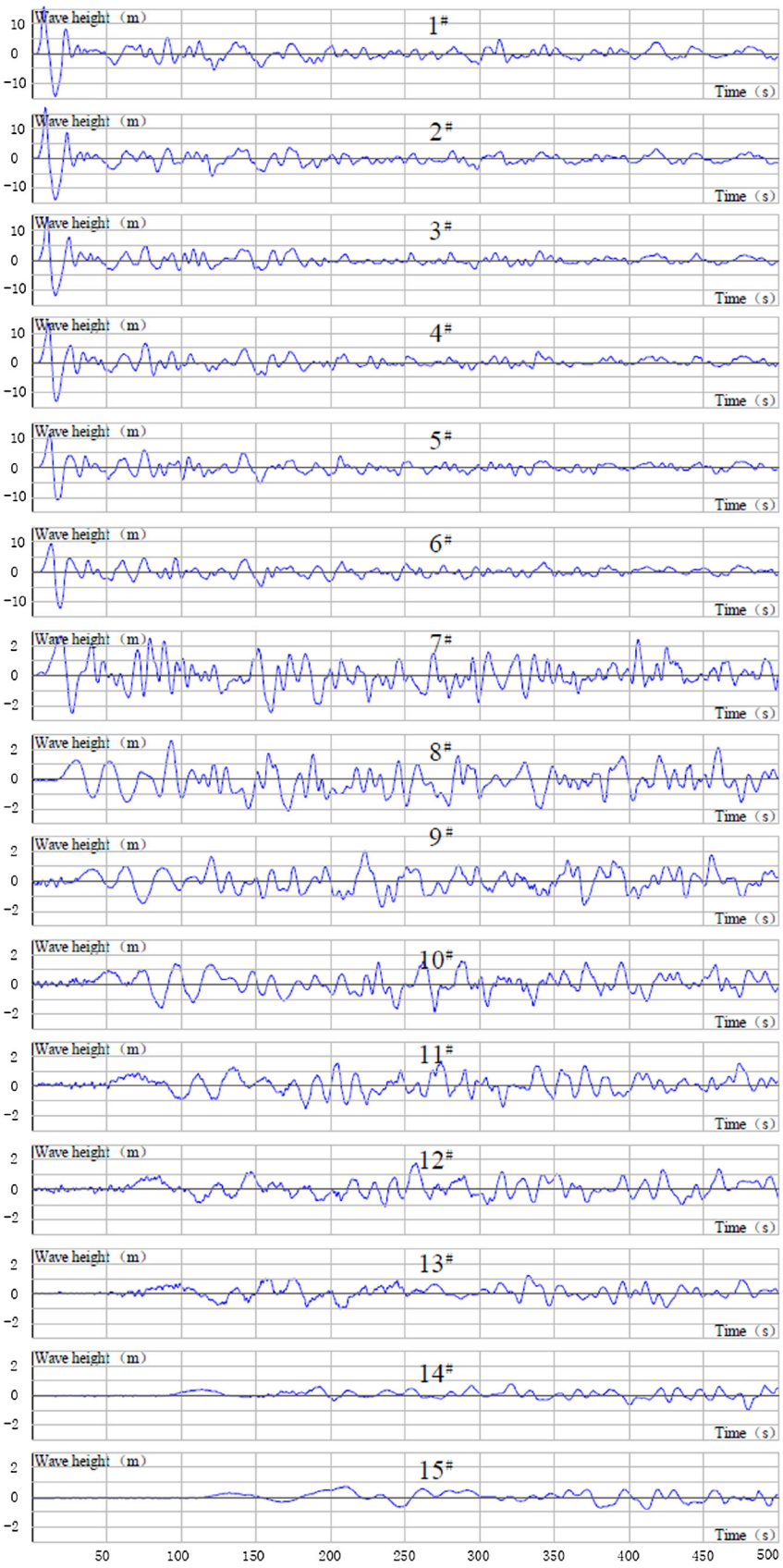

Fig. 14 Gauges data in a 145-m water level experiment

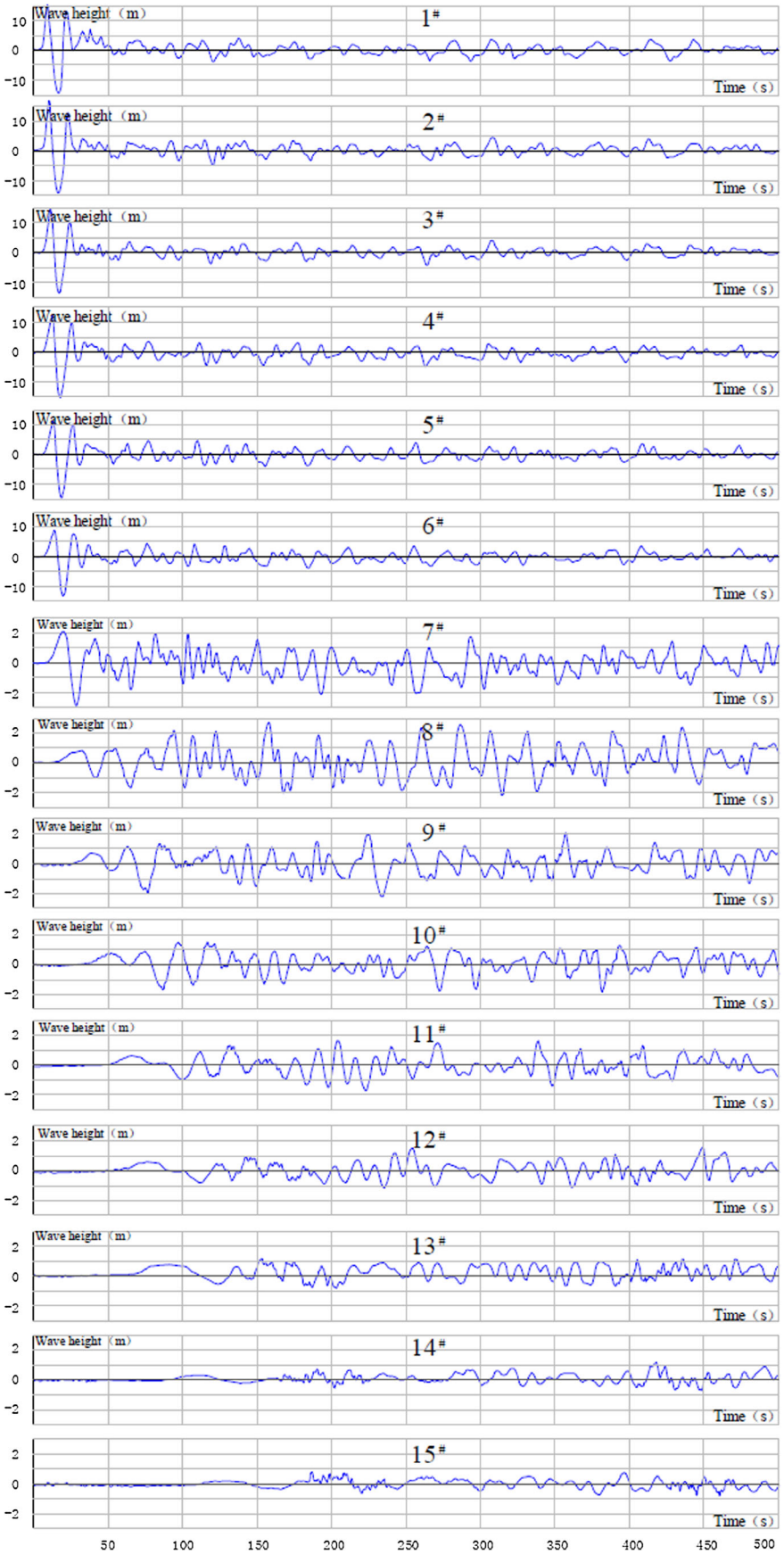

Fig. 15 Gauges data in a 156-m water level experiment

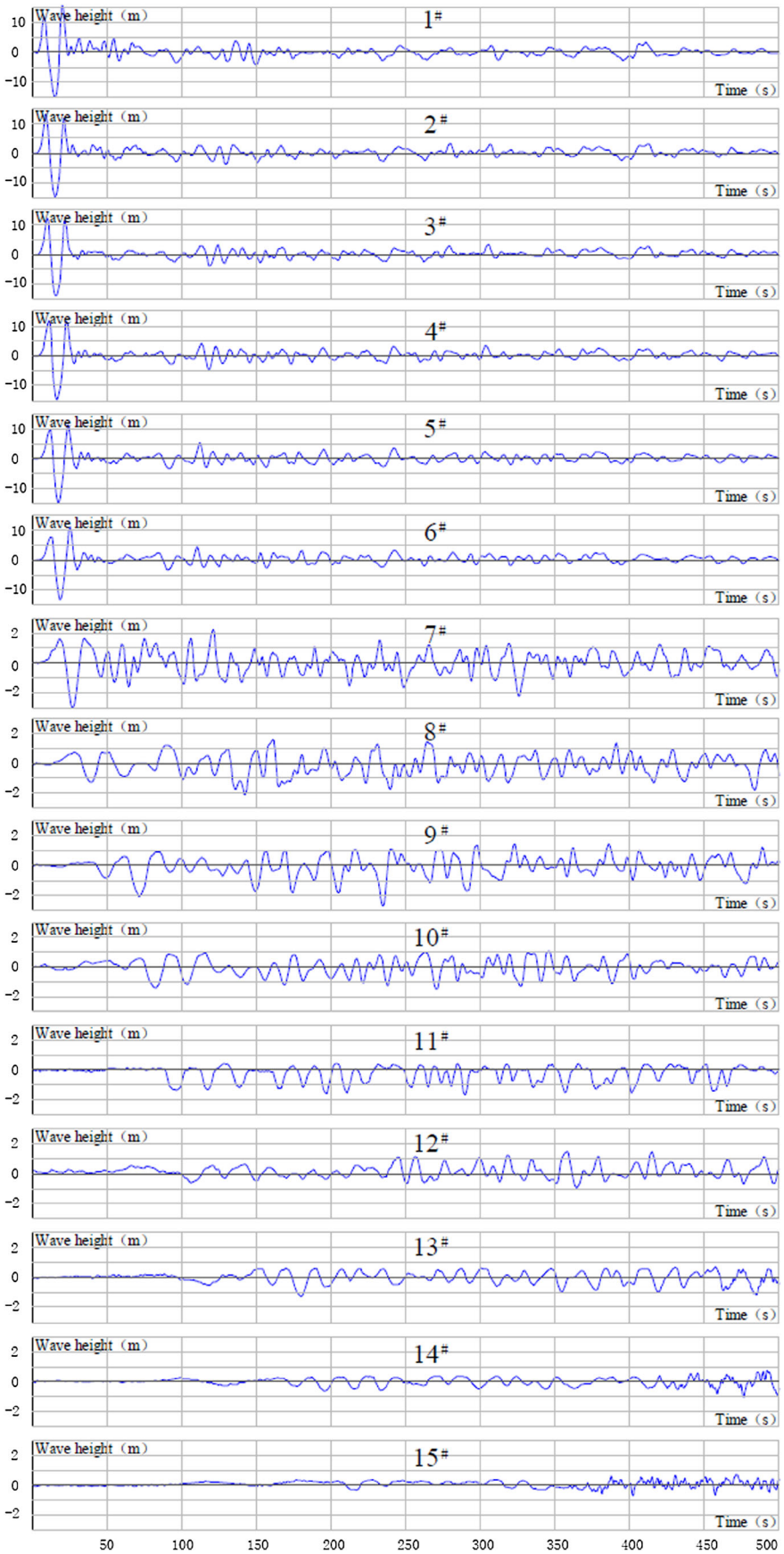

Fig. 16 Gauges data in a 175-m water level experiment

References

Alvarez–Cedrón C, Drempetic V (2009) Modeling of fast catastrophic landslides and impulse waves induced by them in fjords, lakes and reservoirs. Eng Geol 109:124–134

Ataie–Ashtiani B, Nik–Khah A (2008) Impulsive waves caused by subaerial landslides. Environ Fluid Mech 8:263–280

Ball JW (1970) Hydraulic model studies, wave action generated by slides into Mica Reservoir. Technical report. Western Canada Hydraulic Laboratories, Vancouver, Canada

Dai YX, Yin KL, Wang Y (2008) Discussion on method of landslide velocity calculation and surge prediction. Chin J Rock Soil Mech S1:407–411

Davidson DD, Whalin RW (1974) Potential landslide-generated water waves, Libby Dam and Lake Koocanusa, Montana. Technical report. Waterways Experiment Station of U.S. Army Corps of Engineers, Vicksburg

Fritz HM (2002) Initial phase of landslide generated impulse waves. Thesis for the Ph.D, Zürich University

Fritz HM, Hager WH, Minor HE (2001) Lituya Bay case: rockslide impact and wave run–up. Sci Tsunami Hazards 19(1):3–22

Gedik N, Irtem E, Kabdasli S (2005) Laboratory investigation on tsunami run-up. Ocean Eng 32:513–528

Hall JV, Watts GM (1953) Laboratory investigation of the vertical rise of solitary wave on impermeable slopes. Technical report. US Army Corps of Engineers, Beach Erosion Board

Heller V (2007) Landslide generated impulse waves: prediction of near field characteristics. Thesis for the Ph.D Zürich University

Heller V, Hager WH, Minor HE (2009) landslide generated impulse wawes in reservoirs: basics and computation. Technical report. VAW, ETH Zurich

Huang BL, Yin YP, Liu GN, Wang SC, Chen XT, Huo ZT (2012) Analysis of waves generated by Gongjiafang landslide in Wu Gorge, Three Gorges Reservoir, on November 23, 2008. Landslides. doi:10.1007/s10346-012-0331-y

Huber A, Hager WH (1997) Forecasting impulse waves in reservoirs. Proc. 19th Congres Des Grands Barrages. ICOLD 31:993–1005

Hughes SA (1993) Physical models and laboratory techniques in coastal engineering. Adv Series Ocean Eng 7:1–10

Kamphuis JW, Bowering RJ (1970) Impulse waves generated by landslides. Proc. 12th Coastal Engineering Conference, Washington D.C, New York, 1:575–588

Körner HJ (1976) Reichweite und Geschwindigkeit von Bergstürzen und Fliesschneelawinen. Rock Mech 8(4):225–256

Liu SK (1987) Impulsive wave decaying factors study generated by Xintan landslide in Xiling Gorge of Yangtze River. Chin Water Resour Hydropower Eng 9:11–14

Marcello DR, Giorgio B, Andrea P, Paolo DG (2009) Three-dimensional experiments on landslide generated waves at a sloping coast. Coast Eng 56:659–671

Muller D, Schurter M (1993) Impulse waves generated by an artificially induced rockfall in a Swiss lake. Proc. 25th IAHR Congress 4: 209–216

Sander D (1990) Weakly nonlinear unidirectional shallow water waves generated by a moving boundary. Technical report. VAW, ETH, Zurich

Silvia B, Marco P (2011) Shallow water numerical model of the wave generated by the Vajont landslide. Environ Model Softw 26:406–418

Synolakis CE (1991) Generation of long waves in laboratory. Waterway, port, coastal, and ocean engineering. ASCE 116(2):252–266

Ursell F, Dean RG, Yu YS (1960) Forced small amplitude water waves: a comparison of theory and experiment. J Fluid Mech 7:3–52

Wang DY, Liu SK (1986) Xintan landslide impulsive wave survey in June of 1985. Yangtze River 10:24–27

Wang Y, Yin KL (2003) Analysis of movement process of landslide in reservoir and calculation of its initial surge height. Earth Science—J China Univ Geosci 28(5):579–582

Wang Y, Yin KL (2004) Perturbation method of superposing initial surge height of landslide along reservoir shoreline. Chin J Rock Mech Eng 5:717–720

Wang Y, Yin KL (2008) Research on propagat and climb height of surge triggered by landslide in reservoir. Chin J Rock Soil Mech 29(4):1031–1035

Wang YL, Chen FY, Qi HL, Li YB (1994) The effect of rockfall and landslide on channel and the study on the characteristics of surge generated by landslide. Chin J Geol Hazard Control 3:95–100

Wieland M, Gray JM, Hutter K (1999) Channelized free-surface flow of cohesionless granular avalanches in a chute with shallow lateral curvature. J Fluid Mech 392:73–100

Yang J (1987) Some big tsunamis generated by landslide in history. Chinese Northwest Hydropower 2:13

Yin KL, Du J, Wang Y (2008) Analysis of surge triggered by Dayantang landslide in Shuibuya Reservoir of Qingjiang River. Chin J Rock Soil Mech 29(12):3266–3270

B. Huang (✉) · S. Wang · X. Chen · G. Liu
Wuhan Centre of China Geological Survey,
Wuhan, 430205, China
e-mail: bolinhuang79@gmail.com

B. Huang · Y. Yin
China University of Geosciences,
Wuhan, 430074, China

Y. Yin
China Institute for Geo-Environment Monitoring,
Beijing, 100081, China

Z. Jiang
Changjiang River Science Research Institute,
Wuhan, 430010, China

J. Liu
University of Wisconsin—Madison,
Madison, WI, USA